QUARTERLY OF APPLIED MATHEMATICS
JULY 1978

DYNAMICS OF THE JOSEPHSON JUNCTION*

BY

M. LEVI AND F. C. HOPPENSTEADT

Courant Institute, New York University

AND

W. L. MIRANKER

IBM T. J. Watson Research Center, Yorktown Heights,

Abstract. We study the sine-Gordon equation and systems of discrete approximations to it which are respectively a model of the Josephson junction and models of coupled-point Josephson junctions. We do this in the so-called current-driven case. The voltage response of these devices is the average of the time derivative of the solution of these equations and we demonstrate the existence of running periodic solutions for which the average exists. Static solutions are also studied. These together with the running solutions explain the multiple-valuedness in the response of a Josephson junction in several cases. The stability of the various solutions is described in some of the cases. Numerical results are displayed which give details of structure of solution types in the case of a single point junction and of the one-dimensional distributed junction.

1. Introduction. The Josephson junction is a cryogenic device consisting of two super-conductors separated by a thin gap. (A descriptive survey of the Josephson junction may be found in [5] while a more popular description is found in [3].) There is a jump in the electron wave function across the junction gap (see Fig. 1.1). The corresponding jump in the argument of this wave function, denoted by $\phi(x, t)$, satisfies the damped sine-Gordon equation which in appropriate units is (subscripts denote differentiation)

$$\phi_{tt} + \sigma\phi_t - \phi_{xx} + \sin\phi = 0, \qquad 0 \le x \le 1.$$

Two principal cases of interest arise, depending on how the device is driven. In the so-called voltage-driven case, a constant voltage is maintained across the gap, and the resulting current is measured. In the so-called current-driven case, a constant current is maintained flowing across the gap, and the resulting voltage is measured.

Experiments show that the voltage is a multiple-valued function of the current; this, in addition to the junction's extremely short response time and low power dissipation, makes the junction useful for computer circuits.

The voltage-driven case corresponds to the following boundary conditions for ϕ:

$$\phi_t|_{x=0} = V, \qquad \phi_x|_{x=1} = H,$$

* Received November 23, 1977. The authors thank Dr. F. Odeh for informative discussions concerning the problem.

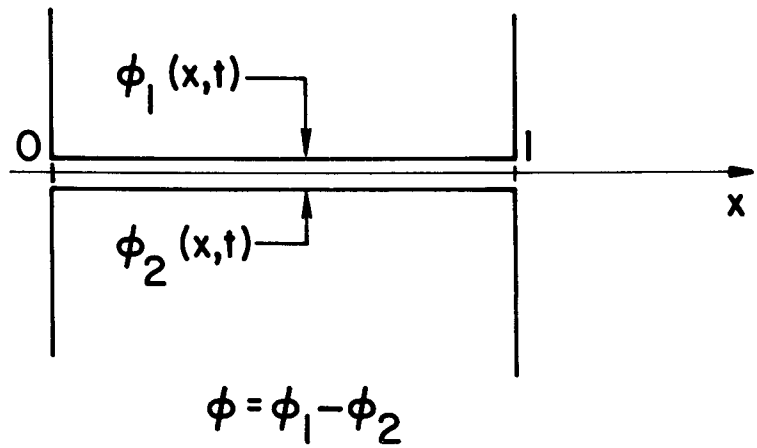

FIG. 1.1 This is a visualization of a Josephson junction. Two superconductors are separated by a thin gap. The model studied here is based on the jump in the electron wave function across the gap, denoted here by ϕ.

where V is the applied voltage and H is an applied magnetic field. The resulting current is determined as a time-average of ϕ_x . The voltage-driven case has been treated elsewhere (see [4] and [6]).

The boundary conditions for the current-driven case are

$$\phi_x|_{x=0} = H, \qquad \phi_x|_{x=1} = H + I,$$

where I is the applied current. The voltage across the gap is $\phi_t(x, t)$. $\phi_t(x, t)$ is typically highly oscillatory, and so time-averages $\langle\phi_t(x, t)\rangle$[1] are actually measured. Such averages exist for solutions whose time-derivatives are periodic. In this paper we present a study of such solutions, for which we henceforth use the term running periodic solution.

In Sec. 2, we consider discrete versions of the model which are obtained by making a discrete spatial approximation to $\partial^2/\partial x^2$. When n is the number of mesh points used in this approximation, we refer to the model as the *n-coupled point junction* model. We give mechanical interpretations to the n-coupled point junction model and to the sine-Gordon equation itself.

The *single point junction* model ($n = 1$) has as a mechanical analogue a pendulum with an applied torque. Since we were unable to find a sufficiently detailed analysis of this model in the literature, we supply one for completeness. One feature of this system of particular interest here is that both stable static states and running periodic solutions (i.e., solutions of the form $\phi = \omega t + p(t)$ where p is periodic in t) can coexist for certain parameter values. This is described in Sec. 3.

In Sec. 4 we give the results of numerical analysis of static solutions, including their stability. These solutions correspond to static states of the sine-Gordon equation. Next, in Sec. 5, we prove the existence of running periodic solutions to the sine-Gordon equation (these are solutions of the form $\phi(x, t) = \omega t + p(x, t)$ where p is periodic in t) and to the n-coupled point junctions in Sec. 5.

In the Appendix we give the proofs of assertions made in Sec 3.

---

[1] If the time-average $\langle\phi_t(x, t)\rangle$ exists, it is in fact independent of x.

2. Discretization and mechanical interpretation. We consider the boundary-value problem

$$\phi_{tt} + \sigma\phi_t - \phi_{xx} + \sin\phi = 0, \tag{2.1}$$

$$\phi_x|_{x=0} = H, \qquad \phi_x|_{x=1} = H + I. \tag{2.2}$$

We also consider a discrete version of this problem: for each n, let $h = 1/n$ and replace $\phi((j - 1/2)h, t)$ by $\phi_j(t), j = 1, \cdots, n$. We introduce the functions $\phi_0(t)$ and $\phi_{n+1}(t)$ which would correspond to $\phi(-h/2, t)$ and $\phi(1 + h/2, t)$ respectively. Now replace the x-derivatives in (2.1) and (2.2) by divided differences. Using the discretization of (2.2) to eliminate ϕ_0 and ϕ_{n+1}, we obtain the following system of the ordinary differential equations:

$$\ddot{\phi} + \sigma\dot{\phi} + A\phi - S(\phi) = b. \tag{2.3}$$

In the case $n = 1$, $\phi = \phi_1$, $A = 1$, $S(\phi) = \sin\phi$ and $b = I$. For $n > 1$,

$$\phi = \begin{bmatrix} \phi_1 \\ \cdot \\ \cdot \\ \cdot \\ \phi_n \end{bmatrix}, \quad S(\phi) = \begin{bmatrix} \sin\phi_1 \\ \cdot \\ \cdot \\ \cdot \\ \sin\phi_n \end{bmatrix}, \quad A = \frac{1}{h^2}\begin{bmatrix} 1 & -1 & & & \\ -1 & 2 & -1 & & \\ & \cdot & \cdot & \cdot & \\ & & -1 & 2 & -1 \\ & & & -1 & 1 \end{bmatrix}, \quad b = \frac{1}{h}\begin{bmatrix} -H \\ 0 \\ \cdot \\ 0 \\ H + I \end{bmatrix}.$$

Here A is an $n \times n$ tridiagonal matrix and ϕ, b are n-vectors.

This system is of independent interest in the study of Josephson junctions: it corresponds to n-coupled point junctions. The case $n = 1$ is referred to as the point junction; the case $n = 2$ as the double junction. (Some properties of the double junction are described in [1, 2].)

The systems (2.1)–(2.2) and (2.3) have simple mechanical interpretations. For (2.3) consider a system of n pendula whose points of suspension are equally spaced along a common horizontal axis (see Fig. 2.1). Each pendulum is constrained to move in a plane perpendicular to this axis. Let ϕ_j be the angle between the rod of the jth pendulum and the

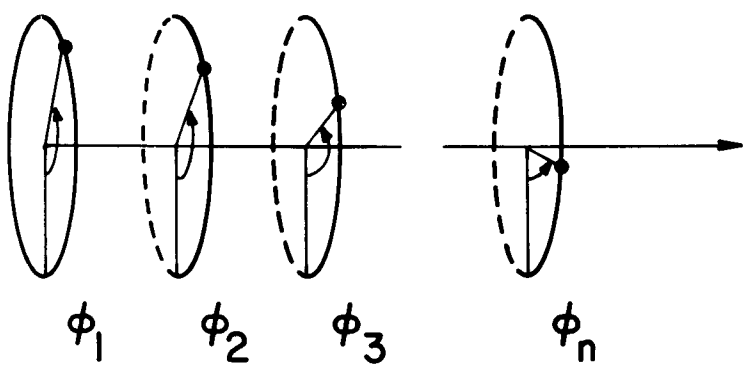

FIG. 2.1 Mechanical analogue of n-coupled point junctions. n pendula are suspended from a common horizontal axis and coupled by an elastic torque. The deviation of each pendulum from equilibrium is denoted by the angles ϕ.

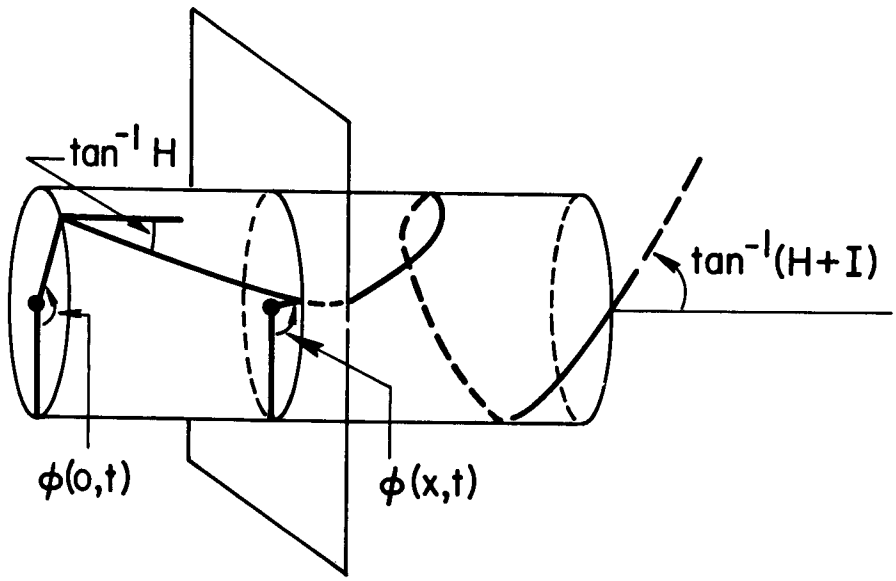

FIG. 2.2 Mechanical analogue of the Josephson junction (see text).

downward-pointing ray. Neighboring pendula are coupled by an elastic torque. In particular, the torque exerted upon the jth pendulum by the $(j+1)$st is $(1/h^2)(\phi_{j+1} - \phi_j)$. The jth pendulum is damped by a torque $\sigma\dot{\phi}_j$. An external torque, H/h, is applied to the first pendulum, while an external torque, $(H+I)/h$, oppositely directed, is applied to the nth pendulum.

These angles ϕ_j satisfy the system (2.3). The point junction corresponds to a single damped pendulum to which an external torque, I, is applied.

The mechanical interpretation of (2.1)–(2.2) consists of an elastic string restricted to lie on the surface of a horizontally placed cylinder of unit length (see Figure 2.2). Each point of the string is constrained to move in a fixed plane perpendicular to the axis of the cylinder. The tension of the string is proportional to its elongation. (This is a continuous analogue of the coupling of the pendula.) x is measured along the axis of the cylinder. From the point x on the axis draw a ray which is perpendicular to the axis and which passes through the string. Let $\phi(x, t)$ be an angle between this ray and the downward pointing ray. The string is subject to a torsional damping, $\sigma\dot{\phi}(x, t)$. Apply a fixed torque H around the axis of the cylinder at one end of the string and a fixed torque $H + I$ oppositely directed at the other end. This angle $\phi(x, t)$ satisfies the system (2.1)–(2.2); moreover, this is so without an approximation based on the requirement that ϕ is small as in the case, say, of the mechanical model of a vibrating string which leads to the wave equation.

3. A single point junction. The single junction corresponds to (2.3) for $n = 1$. Replacing $\phi = \phi_1(t)$ by $x(t)$, we rewrite (2.3) as the following system:

$$\dot{x} = y, \qquad \dot{y} = -\sigma y + I - \sin x. \tag{3.1}$$

The mechanical analogue of this is the damped pendulum with an applied constant torque I. This is a well-studied problem (cf. [9, pp. 70 ff.], and [10]), and in the case $I > 1$ a running periodic solution is known to exist. When $I \leq 1$, the (x, y)-phase plane of (3.1) acquires rest points and yet for certain σ, as we will show, there exists a nontrivial running

solution. Indeed, this solution coexists with static solutions, the latter corresponding to the rest points in the phase plane. This explains the existence of two different values of voltage for a given current.

In Sec. 3.1 we state our results; proofs follow in the Appendix. In Sec. 3.2 we give the results of numerical computations.

3.1 Statement of results. We consider three separate cases: *A*) $I > 1$; *B*) $I = 1$; *C*) $I < 1$ for (3.1). The following are statements of the results for each of the cases. The proofs follow in the Appendix.

PROPOSITION 3.1 (case (*A*); $I > 1$). For any $I > 1$ and $\sigma > 0$, there are no rest points in the phase plane and there exists exactly one running periodic solution which is, moreover, globally exponentially stable, i.e. each trajectory in the phase plane tends to it exponentially as $t \to \infty$.

Since for two solutions (x_1, y_1) and (x_2, y_2) we know that $y_1 - y_2$ tends to zero exponentially, it follows that for the x-coordinates we have

$$x_1(t) - x_2(t) = \text{const} + O(\exp(-\beta t)), \quad \text{as} \quad t \to \infty;$$

i.e. up to a constant shift in phase, these coordinates tend to each other as $t \to \infty$.

The voltage $V = V(\sigma, I) = \langle y_p(t) \rangle$ by definition, where $y_p(t)$ is the time-derivative of the running periodic solution $x_p(t)$. For future reference we note that the relation between the period T of $y_p(t)$ and V is

$$V(\sigma, I) = \langle y_p(t) \rangle = \int_0^T x_p(t)dt \Big/ \int_0^T dt = \frac{2\pi}{T},$$

since, as will be seen, $x_p(t)$ increases monotonically by 2π during the time T.

Remark 3.1. For $I > 1$ and any $\sigma > 0$, $V(\sigma, I)$ is a smooth function of its arguments, monotone decreasing in σ and increasing in I (see Fig. 3.1). This fact is demonstrated in the Appendix.

PROPOSITION 3.2 (case (B); $I = 1$). If $I = 1$, there exists a critical $\sigma_0 > 0$ such that:

(i) For $0 < \sigma < \sigma_0$ there exists an exponentially stable running periodic solution. The phase portrait of the system is shown in Fig. 3.2(i) with the domains of attraction of singular points shaded.

(ii) For $\sigma > \sigma_0$ every solution tends to one of the singular points (see Fig. 3.2(ii)).

(iii) For the (exceptional) case $\sigma = \sigma_0$ the phase plane is split into two regions (see Fig. 3.2(iii)). The boundary between these regions is made up of the trajectories that connect up two neighboring singular points; the trajectories from the upper region tend to this boundary, while trajectories from the lower region tend to the singular points.

PROPOSITION 3.3 (case (c); $I < 1$). For $I < 1$ the situation is similar to the previous case. There exists $\sigma = \sigma_0(I)$ such that:

i) For $0 < \sigma < \sigma_0(I)$ there exists a unique exponentially stable running periodic solution.

ii) For $\sigma > \sigma_0(I)$ there is no running periodic solution, and every trajectory in the phase plane tends to one of the rest points.

iii) For $\sigma = \sigma_0(I)$ the phase plane is split into two regions: all trajectories in the upper region tend to the boundary between the two regions. Every trajectory in the lower region tends to one of the rest points.

The results of Propositions 3.1-3.3 are illustrated in Fig. 3.3. The proofs of the assertions made here are given in the Appendix.

3.2 Numerical experiments. The results of numerical experiments for the point junction

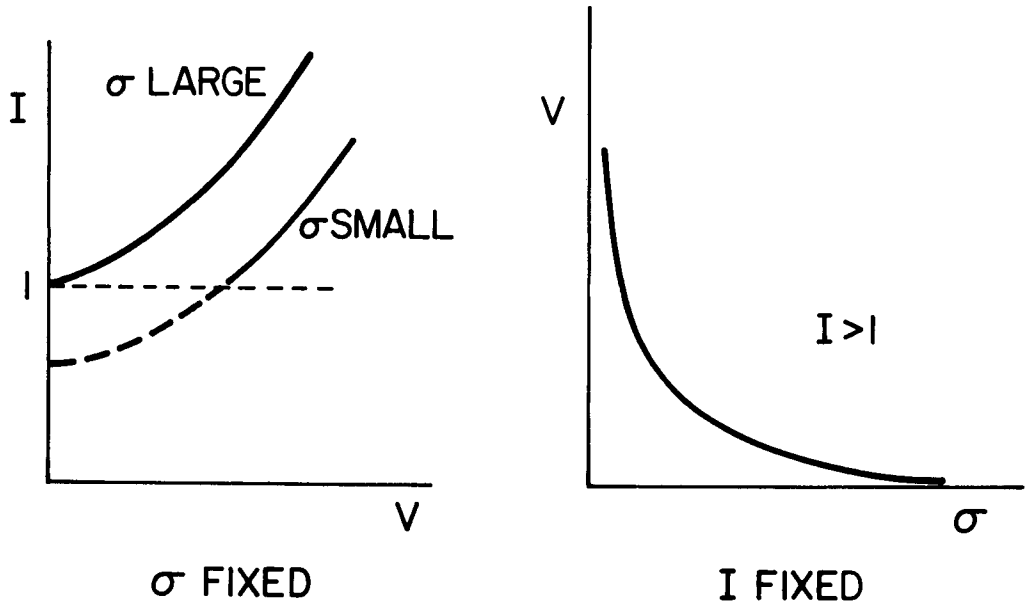

FIG. 3.1 The dependence of $V(\sigma, I)$ on the parameters σ and I is described here. The dashed line arising for σ small and $I < 1$ indicates that the response is multivalued, as is discussed in Proposition 3.3.

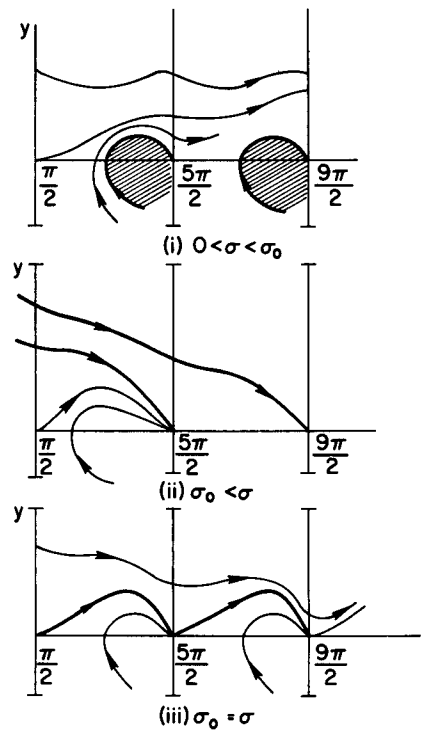

FIG. 3.2 Phase plane diagram corresponding to proposition 3.2 ($I = 1$). The notation $y_h(x)$ is introduced and used in the proof of Proposition 3.2 (see Appendix).

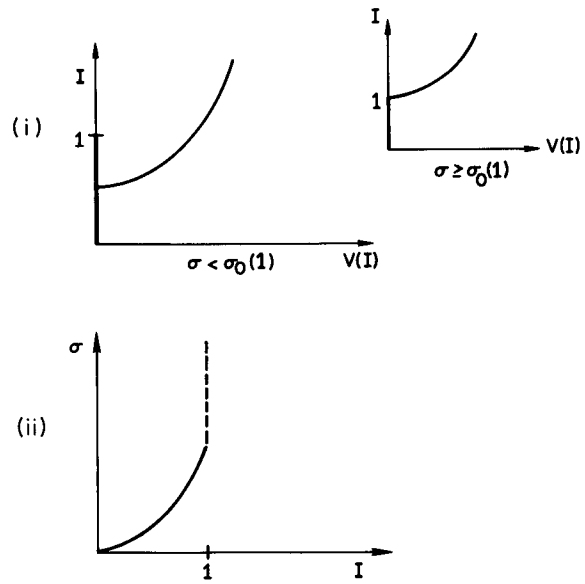

FIG. 3.3 *I-V* diagrams in case (C) ($I < 1$) (i) shows that the response is multivalued for some values of the applied torque (I) if $\sigma < \sigma_0(1)$; (ii) gives the dependence of σ on I.

are displayed here. In Fig. 3.4 we plot I against $V = 2\pi/T$ for various values of σ, the current-voltage curves of the point function. In Fig. 3.5 we plot $\sigma = \sigma_0(I)$. In mechanical terms, for a given torque I, $\sigma_0(I)$ is the critical value of damping below which a running periodic solution may be sustained.

4. Static states in current-driven junctions. The static states of the current-driven junction are determined as solutions $\phi = u(x)$ of the problem

$$u_{xx} = \sin u, \qquad u_x(0) = H, \qquad u_x(1) = H + I.$$

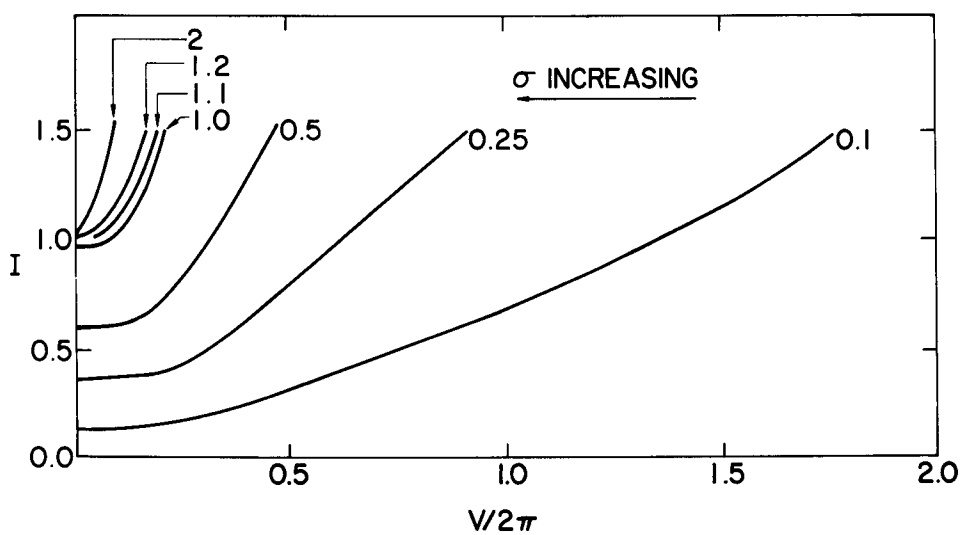

FIG. 3.4. Numerical calculation of the *I-V* diagrams for various choices of σ.

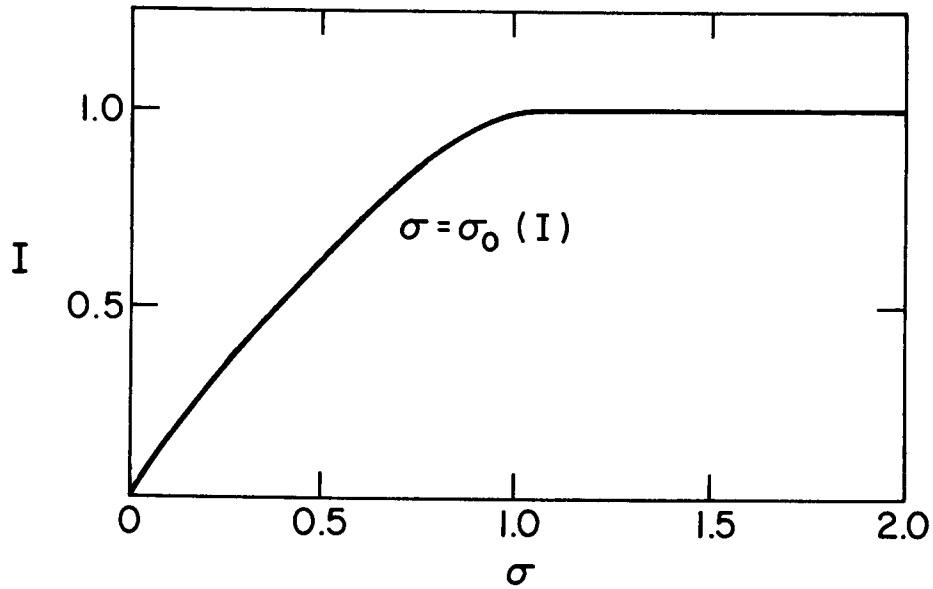

FIG. 3.5. Numerical calculation of $\sigma = \sigma_0(I)$.

One approach to this problem is to obtain the solution to the differential equation in terms of elliptic integrals and then determine which among these solutions satisfy the boundary conditions (see [7]). This approach ultimately leads to a form for solutions that can be rigorously justified and that can be evaluated numerically.

Rather than this analytic approach, we take a direct numerical approach that provides a description of static states as well as their stability as solutions to the sine-Gordon equation.

4.1 Static states. The phase portrait of the static state equation is given in Fig. 4.2. In this figure, particular values for H and I are indicated by the labelled horizontal lines. Solutions of the boundary-value problem are those that start on the line $u_x = H$ for $x = 0$ and lie on the line $u_x = H + I$ for $x = 1$. The numerical scheme presented here is based on this fact.

The numerical solution proceeds in the following way. First, we fix a value for $H \geq 0$.

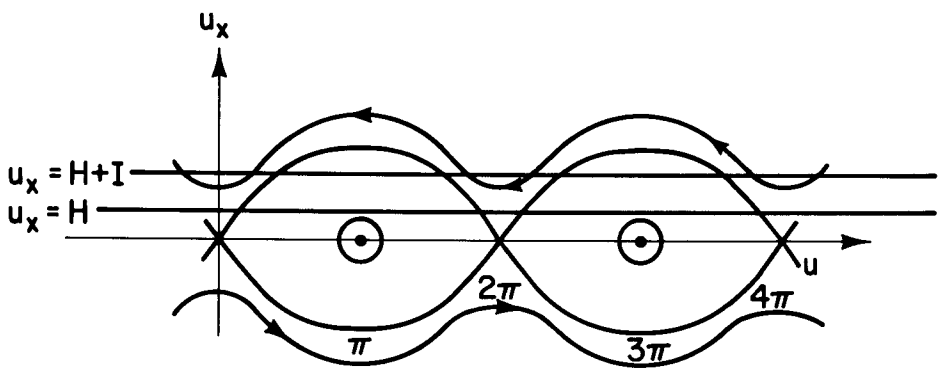

FIG. 4.1. Phase plane description of solutions to the static state problem. A solution must start on the line $u_x = H$ and end on the line $u_x = H + I$.

Then an initial point on the line $u_x = H$ is selected; call the u-coordinate of this point $u(0)$. Next, the initial-value problem

$$u_{xx} = \sin u, \qquad u(0) = u(0), \qquad u_x(0) = H,$$

is solved for $0 \leq x \leq 1$. The terminal value, $u_x(1)$, then gives the value of I for which the computed solution satisfies the right-hand boundary condition:

$$I = u_x(1) - H.$$

By repeating this procedure for many values of $u(0)$, $0 \leq u(0) \leq 2\pi$, we obtain a relation between I and $u(0)$ for each choice of H. The results of the calculations are summarized in the bifurcation diagram in Fig. 4.1. These diagrams show that for each value of H, there is an interval of I values, $0 \leq I \leq I_{\max}(H)$, for which there are two static states. For I greater than $I_{\max}(H)$, there are no static states (see Fig. 4.2).

$I_{\max}(H)$ is plotted in Fig. 4.3. A critical experiment performed by Rowell [8] that clinched the identification of the observed resistanceless current in the junction as the d.c.-Josephson effect gave $I_{\max}$ as a function of H. These preliminary calculations presented here agree with Rowell's observations.

4.2 Stability of the static states. The stability of each static state can be determined from the linearization of the sine-Gordon equation. Let H and I be fixed ($0 \leq I \leq$

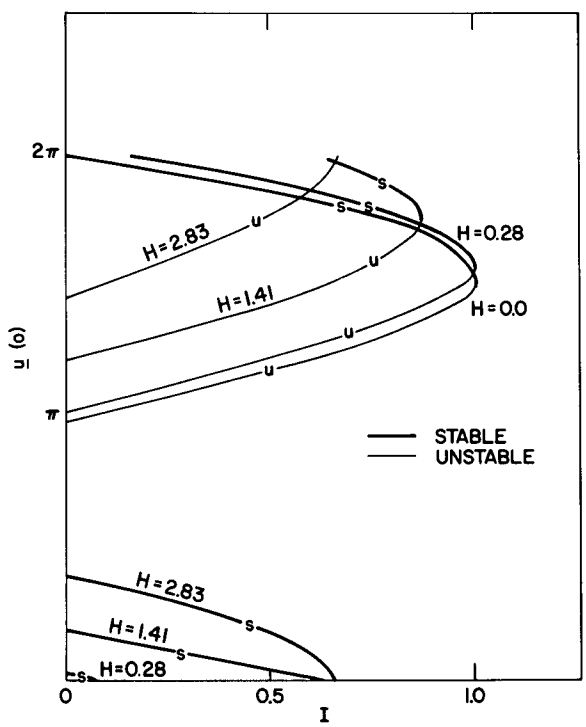

FIG. 4.2. This diagram describes the static states and their stability. Branches labelled S are stable, those labelled U are unstable. For example, for $I = .5$ and $H = 2.83$, there are two static states, one beginning near the point $(\pi/4, H)$, the other near $(2\pi - \pi/4\ H)$. The former one is stable, the latter one is unstable. This figure shows the dependence of $I_{\max}(H)$, the maximum current for which a static state is found, on H the applied magnetic field.

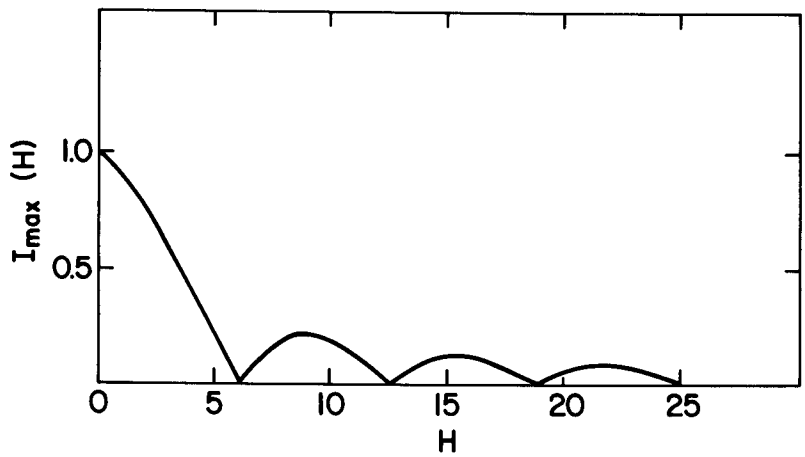

FIG. 4.3.

$I_{\max}(H)$), and let $u^*(x)$ be a corresponding static state. The linearization of the problem about this state is

$$\tilde{\phi}_{tt} + \sigma\tilde{\phi}_t - \tilde{\phi}_{xx} = \cos(u^*(x))\tilde{\phi},\ \tilde{\phi}_x(0, t) = 0,\ \tilde{\phi}_x(1, t) = 0.$$

Setting $\tilde{\phi} = \exp(pt)V(x)$, we have the problem

$$V_{xx} + \cos(u^*(x))V = \lambda V,\ V_x(0) = V_x(1) = 0,$$

for V, where $\lambda = p^2 + p\sigma$. The largest eigenvalue of this problem is easily determined numerically by using the Rayleigh quotient.

Since $p = -(\sigma/2) \pm ((\sigma^2/4) + \lambda)^{1/2}$, if $\lambda > 0$, then $\operatorname{Re} p > 0$, but if $\lambda < 0$, then $\operatorname{Re} p < 0$. In Fig. 4.2, the branches labelled s (stable) are those for which we found $\lambda < 0$; those labelled u (unstable) are those for which we found $\lambda > 0$.

5. Discrete ($n \geq 2$) and continuous junctions. As we mentioned in the introduction, the existence of a stationary voltage is assured by the existence of a running periodic solution. In this section we prove the existence of such a solution for both the discrete ($n \geq 2$) and continuous cases. However we deal here only with $I > 1$ since the case $I \leq 1$ is open.

We formulate our results in the following

THEOREM 5.1. If $I > 1$, then the systems

$$\ddot{\phi} + \sigma\dot{\phi} + A\phi + \sin\phi = b, \tag{5.1a}$$

$$\phi_{tt} + \sigma\phi_t - \phi_{xx} + \sin\phi = 0, \tag{5.1b}$$

$$\phi_x(0, t) = H,\ \phi_x(1, t) = H + I,$$

each have at least one running periodic solution.

Remark 5.1. F. Odeh shows the stability of running periodic solutions of (5.1b) in the voltage-driven case (see [6]). His argument carries over to the current-driven case, although the proof presented here takes a different point of view. The remainder of this section is devoted to the proof of this proposition.

Proof of Theorem 5.1. Part a). First we consider $n = 2$, the double junction, and then $n > 2$.

$n = 2$. The system under consideration is

$$\begin{aligned} \ddot{\phi}_1 + \sigma\phi_1 + \tfrac{1}{4}(\phi_1 - \phi_2) + \sin\phi_1 &= -2H, \\ \ddot{\phi}_2 + \sigma\phi_2 + \tfrac{1}{4}(\phi_2 - \phi_1) + \sin\phi_2 &= 2(H + I). \end{aligned} \tag{5.2}$$

We rewrite (5.2) in terms of $x = \phi_2 - \phi_1$, $y = \frac{1}{2}(\phi_2 + \phi_1)$ (y being a center of mass coordinate):

$$\begin{aligned} &\text{a)} \quad \ddot{x} + \sigma\dot{x} + \tfrac{1}{2}x + \sin\phi_2 - \sin\phi_1 = 2(2H + I), \\ &\text{b)} \quad \ddot{y} + \sigma\dot{y} + \tfrac{1}{2}(\sin\phi_1 + \sin\phi_2) = I. \end{aligned} \tag{5.3}$$

(A system of this form for the double Josephson junction appears in [1] and [2].) (5.3) is in turn written as the following first-order system:

$$\begin{aligned} &\text{a)} \quad \dot{x} = u, \\ &\text{b)} \quad \dot{u} = -\sigma u - \tfrac{1}{2}x + \sin\phi_1 - \sin\phi_2 + 2(2H + I), \\ &\text{c)} \quad \dot{y} = v, \\ &\text{d)} \quad \dot{v} = -\sigma v - \tfrac{1}{2}(\sin\phi_1 + \sin\phi_2) + I. \end{aligned} \tag{5.4}$$

(5.3b) can be rewritten as

$$\frac{d}{dt}(\exp(\sigma t)\dot{y}) = (I - \tfrac{1}{2}(\sin\phi_1 + \sin\phi_2))\exp(\sigma t) \equiv c(t)\exp(\sigma t) \geq c_0 \exp(\sigma t),$$

for some $c_0 > 0$ (since $I > 1$).

If $\dot{y}_0 \equiv \dot{y}(0) \geq 0$, then for $t > 0$

$$\exp(\sigma t)\dot{y}(t) = \dot{y}_0 + \int_0^t \exp(\sigma t)c(t)dt \geq c_0(\exp(\sigma t) - 1),$$

i.e.

$$\dot{y}(t) \geq c_0(1 - \exp(-\sigma t)), \qquad t \geq 0. \tag{5.5}$$

That is, $y(t)$ is monotone increasing for $t > 0$ if $I > 1$ and $\dot{y}(0) \geq 0$.

Consider a solution of the system (5.4) which starts at a point $(x_0, 0, u_0, v_0)$ on the half-hyperplane $\{y = 0, v \geq 0\}$ at $t = 0$ (see Fig. 5.1). According to (5.5), this solution will intersect the half-hyperplane in $\mathbf{R}^4$, $\{y = 2\pi l, v \geq 0\}$ (l an integer to be chosen later) transversally, i.e. there exists $T = T(x_0, u_0, v_0)$ such that

$$\begin{aligned} y(T, x_0, u_0, v_0) &= 2\pi l, \\ \dot{y}(T, x_0, u_0, v_0) &> 0. \end{aligned} \tag{5.6}$$

By the implicit function theorem and the theorem on dependence of a solution on initial data, (5.6) implies that

$$T = T(x_0, u_0, v_0)$$

is a continuous (even smooth) function. Thus we have a continuous map

$$M: (x_0, u_0, v_0) \to (x(T), u(T), v(T))$$

with $T = T(x_0, u_0, v_0)$ defined by (5.6) from $R_+^3 = \{(x, u, v); v \geq 0\}$ into itself. Take a

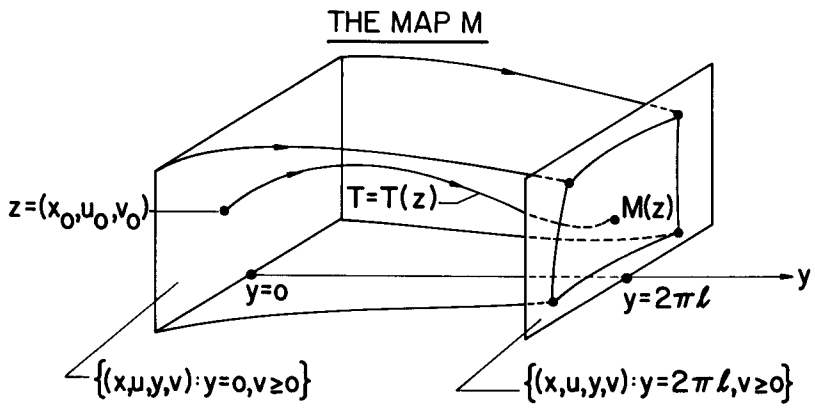

FIG. 5.1. The map M. This is used in the proof of Theorem 5.1.

parallelepiped in R_+^3 (see Figure 5.1) defined by

$$P = \{(x, u, v), v \geq 0, \max(|x|, |u|, v) < c\},$$

with an appropriate choice of c (depending on σ) to be made later. We will show that

$$MP \subset P. \tag{5.7}$$

This would prove the existence of a fixed point of the map M (by the Bohl-Brouwer theorem), and hence the existence of a running periodic solution for Eq. (5.3) and hence for (5.2).

Indeed, if for some $P = (x_0, u_0, v_0)$, $M(P) = P$, i.e.

$$x(T; x_0, 0, u_0, v_0) = x_0, \qquad y(T; x_0, 0, u_0, v_0) = 2\pi l,$$
$$u(T; x_0, 0, u_0, v_0) = u_0, \qquad v(T; x_0, 0, u_0, v_0) = v_0,$$

then from the definition of x and y,

$$\phi_1(T) = \phi_1(0) + 2\pi l, \ \phi_2(T) = \phi_2(0) + 2\pi l,$$
$$\dot{\phi}_1(T) = \dot{\phi}_1(0), \qquad \dot{\phi}_2(T) = \dot{\phi}_2(0).$$

This shows the existence of a running periodic solution. It remains therefore, to demonstrate (5.7). First choose c so that (see (5.4d)) $-\sigma c + 1 + I < 0$, i.e. take any

$$c > \frac{I + 1}{\sigma} \equiv c_0.$$

(Occasionally different constants whose exact value is not important will be denoted by the same symbol.) This guarantees that no matter what x, y and v are, $\dot{v} < 0$ on the boundary of P (with the indicated choice of c), so that the v-projection of P goes into itself. To cause the same to be true for the (x, u)-projection, we have to choose a constant c so large that the damping effect brings $|x|, |u| \leq c$ into itself.

Any solution of (5.3a) can be written by the variation of constants formula in the (implicit) form

$$x(t) = c_1 \exp(\lambda_1 t) + c_2 \exp(\lambda_2 t) + \frac{1}{\lambda_2 - \lambda_1}\int_0^t \exp(\lambda_2(t - \tau) f(\tau) d\tau$$
$$+ \frac{1}{\lambda_1 - \lambda_2}\int_0^t \exp(\lambda_1(t - \tau) f(\tau) d\tau, \tag{5.8}$$

where $f(t) = 2(2H + I) + \sin \phi_1 - \sin \phi_2$, and

$$\lambda_{1,2} = -\frac{\sigma}{2} \pm \left(\frac{\sigma^2}{4} - 1/2\right)^{1/2}$$

are the characteristic roots. (We assume that $\lambda_1 \neq \lambda_2$, i.e. $\sigma^2 \neq 2$; this exceptional case can be treated analogously and is omitted.) (5.8) also gives

$$u(t) = \dot{x}(t) = c_1\lambda_1 \exp(\lambda_1 t) + c_2\lambda_2 \exp(\lambda_2 t) + \frac{\lambda_2}{\lambda_2 - \lambda_1}\int_0^t \exp(\lambda_2(t-\tau)f(\tau)d\tau$$
$$+ \frac{\lambda_1}{\lambda_1 - \lambda_2}\int_0^t \exp(\lambda_1(t-\tau))f(\tau)d\tau. \tag{5.9}$$

Because of the bound on $f(\tau)$ and since $\operatorname{Re}\lambda_i < 0$, $i = 1, 2$ ($\sigma > 0$), it is easy to see that the last two terms in both (5.8) and (5.9) are bounded for all $t \geq 0$, whereas the first two terms in both expressions tend to zero as t increases. Choose a constant $A > 0$ and larger than any of the last two terms in (5.8) and (5.9), and increase c, if necessary, so that $c \geq 3A$.

We claim that there exists $\tau = \tau(c)$ such that for all $t > \tau$, $|x(t)| < c$, $|u(t)| < c$, if initially $|x(0)| \leq c$, $|u(0)| \leq c$.

If l in (5.6) is chosen large enough, then

$$T(z) = T(x_0, u_0, v_0) > \tau(c)$$

for all $z \in \mathbb{R}_+^3$. (This last assertion follows directly from (5.5).) Then the (as-yet unproved) claim and the last inequality assures us that $MP \subset P$.

To show the existence of the required τ, take $|x(0)| \leq c$, $|u(0)| \leq c$.
Then (5.8), (5.9) imply that

$$|c_1 + c_2| \leq C, \qquad |c_1\lambda_1 + c_2\lambda_2| \leq C.$$

Then

$$|c_1| \leq \frac{C(|\lambda_2| + 1)}{|\lambda_2 - \lambda_1|}, \qquad |c_2| \leq \frac{C(|\lambda_1| + 1)}{|\lambda_2 - \lambda_1|}.$$

Thus c_1, c_2 are bounded independently of the choice of $x(0)$ and $u(0)$ (within the permitted range). Thus, since $\operatorname{Re}\lambda_i < 0$, $i = 1, 2$,

$$|c_1 \exp(\lambda_1 t) + c_2 \exp(\lambda_2 t)| < A,$$
$$|c_1\lambda_2 \exp(\lambda_1 t) + c_2\lambda_2 \exp(\lambda_2 t)| < A,$$

for $t > \tau(C)$ properly chosen.

Finally, (5.8) and (5.9) together with previous remarks imply

$$|x(t)| < A + A + A \leq c, \qquad |u(t)| < A + A + A \leq c,$$

which completes the case $n = 2$ of part *a*) of Theorem 5.1.

The case $n > 2$ of part *a*) to which we now turn is similar. Introduce a new variable (center of mass)

$$\xi = \frac{1}{n}(\phi_1 + \cdots + \phi_n);$$

the equation for ξ is

$$\ddot{\xi} + \sigma\dot{\xi} = -\frac{1}{n}\Sigma \sin \phi_k + I \qquad (nh = 1). \tag{5.10}$$

Take the deviation of ϕ from ξ as another variable:

$$\psi_k = \phi_k - \xi; \tag{5.11}$$

the equation for $\psi = (\psi_1, \cdots, \psi_2)^T$ is

$$\ddot{\psi} + \sigma\dot{\psi} + A\psi = N(\psi + e\xi) \tag{5.12}$$

where

$$e = \begin{matrix} 1 \\ \vdots \\ 1 \end{matrix}, \quad N(\psi + e\xi) = N(\phi) = -e\left(I - \frac{1}{n}\Sigma \sin \phi_k\right) - \sin \phi + b.$$

All we need to know about N is its boundedness and the fact that $\Sigma N_k = 0$; note also, that $\Sigma\psi_k = 0$ by definition. Thus it is natural to restrict (5.12) to the hyperplane $\Sigma\psi_k = \Sigma\dot{\psi}_k = 0$. The system (5.10), (5.12) with this restriction is equivalent to (2.3). Exactly as in the case of a double junction, we see that (5.10) implies $\dot{\xi}(t) > 0$ if $I > 1$ and $\dot{\xi}(0) \geq 0$. Write the system (5.10), (5.12) in the form

$$\begin{aligned} &\dot{\xi} = \eta, \eta = -\sigma\xi + I - \frac{1}{n}\Sigma \sin (\xi + \psi_k), \\ &\dot{\psi} = \chi, \dot{\chi} = -\sigma\chi - A\psi + N(\psi + e\xi). \end{aligned} \tag{5.13}$$

Take the set

$$S_0 = \{(\xi, \eta, \psi, \chi) \in \mathbb{R}^{2n+2}: \xi = 0, \eta \geq 0, \sum \psi_k = \sum \chi_k = 0\}$$

homeomorphic to $\mathbb{R}_+^{2n-1}$ ($2n$-1-dimensional Euclidean halfspace) and let the solution of (5.13) start on S_0 at $t = 0$.

Since $\dot{\xi}(t) = \eta(t) > 0$ ($t > 0$), the trajectories of (5.13) will intersect any hyperplane $\xi = 2\pi l$ ($l > 0$) transversally, so that we have a continuous map of S_0 into

$$S_{2\pi l} = \{(\xi, \eta, \psi, \chi) \in \mathbb{R}^{2n+2}: \xi = 2\pi l, \eta \geq 0, \sum \psi_k = \sum \chi_k = 0\}.$$

We choose an integer l, and we identify S_0 and $S_{2\pi l}$ with $\mathbb{R}_+^{2n+1}$ in an obvious manner.

Then, if M has a fixed point, (5.1a) has a running periodic solution, as is easily checked. To prove the existence of a fixed point, we will show that there exists a natural number l and a constant R, suitably large, so that the subset of S_0 homeomorphic to a ball, namely

$$\{(\eta, \psi, \chi): 0 \leq \eta \leq R, |\psi|, |\chi| \leq R\},$$

maps into itself under M. In other words, it is enough to show that if the solution starts at

$$\xi(0) = 0, \qquad 0 \leq \eta(0) \leq R, \qquad |\psi(0)| \leq R, \qquad |\chi(0)| \leq R,$$

then for $\xi(T) = 2\pi l$ ($T = T(\eta(0), \psi(0), x(0))$) we have

$$0 \leq \eta(T) \leq R, \qquad |\psi(T)| \leq R, \qquad |\chi(T)| \leq R.$$

For the first two equations in (5.13) the proof proceeds exactly as in the double-junction case.

We simplify the last two equations of (5.13), i.e. (5.12), by setting $\psi = Px$, where P diagonalizes A:

$$P^{-1}AP = D.$$

We get

$$\ddot{x} + \sigma\dot{x} + Dx = M,\ M = P^{-1}N.$$

This decouples the linear part of (5.12):

$$\ddot{x}_k + \sigma\dot{x}_k + \mu_k x = M_k, \tag{5.14}$$

where $|M_k| < \alpha$, α some constant.

The μ_k are the eigenvalues of A; one of them, corresponding to the eigenvector

$$v_1 = \begin{bmatrix} 1 \\ \vdots \\ 1 \end{bmatrix},$$

is zero; say $\mu_1 = 0$. The rest of the μ_k are nonzero, which follows by noting that A has only one eigenvector with zero eigenvalue (as is easy to check) and that for symmetric matrices the multiplicity of an eigenvalue coincides with the dimension of its eigenspace. Moreover, $\mu_k > 0$ for $k \geq 2$, using a theorem of Gershgorin.

In terms of our new variable x it suffices to show that if R is sufficiently large, there exists a τ such that if

$$|x(0)| \leq \frac{R}{|P^{-1}|},\ |\dot{x}(0)| \leq \frac{R}{|P^{-1}|}, \tag{5.15a}$$

then

$$|x(t)| \leq \frac{R}{|P|},\ |\dot{x}(t)| \leq \frac{R}{|P|} \quad \text{for} \quad t > \tau. \tag{5.15b}$$

This would imply that the indicated subset of S_0 is mapped into itself and thus complete the proof: indeed,

$$|\psi(0)| \leq R \Rightarrow |x(0)| \leq \frac{R}{|P^{-1}|} \Rightarrow |x(T)| \leq \frac{R}{|P|} \Rightarrow |\psi(T)| \leq R.$$

The same is true for $x = \dot{\psi}$. Here $T = T(z) > \tau$ is assured if we choose l large enough.

Write x_k from (5.14) as

$$x_k(t) = c_k{}^1 \exp(\lambda_k{}^1 t) + c_k{}^2 \exp(\lambda_k{}^2 t) + \frac{1}{\lambda_k{}^1 - \lambda_k{}^2}\int_0^t \exp(\lambda_k{}^1(t-\tau))M_k\, d\tau$$

$$+ \frac{1}{\lambda_k{}^2 - \lambda_k{}^1}\int_0^t \exp(\lambda_k{}^2(t-\tau)M_k\, d\tau,$$

$$\dot{x}_k(t) = c_k{}^1\lambda_k{}^1 \exp(\lambda_k{}^1 t) + \cdots.$$

The $\lambda_k{}^{1,2}$ are the roots of

$$\lambda^2 + \sigma\lambda + \mu_k = 0.$$

For $k \geq 2$, $Re\, \lambda_k^{1,2} < 0$.

To observe the validity of (5.15), we note that the relation $\sum \psi_k = \sum \dot{\psi}_k = 0$ becomes the following relation for x:

$$0 = \sum_k \psi_k = \sum_k \sum_j P_{kj} x_j = \sum_k (cx_1 + \sum_{j \geq 2} P_{kj} \mid x_j) = \mathrm{cn} x_1 + \sum \alpha_k x_k .$$

Here we used the fact that the first column of P is

$$\begin{bmatrix} c \\ \vdots \\ c \end{bmatrix} (\neq 0)$$

an eigenvector corresponding to $\mu_1 = 0$.

Thus x_1 is a linear combination of x_k, $k \geq 2$, and an argument similar to the one in the double-junction case (namely the use of the decay of exponential terms and the boundedness of the integrals) shows (5.15).

This completes the case $n > 2$ and the proof of part *a*) of Theorem 5.1.

Part b). We turn now to the proof for the system (5.1*b*). We omit details similar to the discrete case in part *a*). We begin by integrating the partial differential equation in (5.1*b*) with respect to x; then, using the boundary conditions in (5.1*b*), we get

$$s_{tt} + \sigma s_t = I - \int_0^1 \sin \phi \, dx, \tag{5.16}$$

where

$$s(t) = \int_0^1 \phi(x, t) \, dx.$$

Set

$$\Delta(x, t) = \phi(x, t) - s(t);$$

Δ obeys the following equation and boundary condition:

$$\Delta_{tt} + \sigma \Delta_t - \Delta_{xx} + \sin(\Delta + s) - \int_0^1 \sin(\Delta + s) dx + I = 0, \tag{5.17}$$

$$\Delta_x \big|_{x=0,1} = H, H + I. \tag{BC1}$$

As in part *a*), to show the existence of a running periodic solution of (5.1*b*) it suffices to prove the existence of $T > 0$, $s(0)$, $\dot{s}(0)$, $\Delta(x, 0)$ $\dot{\Delta}(x, 0)$ such that

$$s(T) = s(0) + 2\pi l, \qquad \dot{s}(T) = \dot{s}(0), \qquad \Delta(x, T) = \Delta(x, 0), \qquad \dot{\Delta}(x, T) = \dot{\Delta}(x, 0).$$

Again we introduce a map M. Here

$$M: \begin{bmatrix} \dot{s}(0) \\ \Delta(x, 0) \\ \dot{\Delta}(x, 0) \end{bmatrix} \to \begin{bmatrix} \dot{s}(T) \\ \Delta(x, T) \\ \dot{\Delta}(x, T) \end{bmatrix} \tag{5.18}$$

from

$$s = 0, \qquad \dot{s} \geq 0,$$

$$\Delta_0, \dot{\Delta}_0 \in C^2(0, 1), \text{ with } \Delta_0 \text{ subject to (BC1)}$$

into the set of the same form except that $s = 2\pi l$. Here T is determined by

$$s(\dot{s}_0, \Delta_0, \dot{\Delta}_0, T) = 2\pi l, \tag{5.19}$$

where the integer l is to be chosen later.

Since $I > 1$, (5.16) shows that $\dot{s}(T) > 0$ for any T and any initial data lying in our class ($\dot{s}(0) \geq 0$). Thus (5.19) determines T as a continuous functional of $(\dot{s}_0, \Delta_0, \Delta_0)$. Here we use the fact that s is a continuous functional of its arguments which follows from the continuous dependence of the solution of (5.1b) on its initial data in the $C(0, 1)$-norm.

Thus the map M is well-defined and continuous. It remains to show that M has a fixed point. To do that, we restrict the set of initial data to a compact convex subset K of $\mathbb{R}_+ \times C^{(2)} \times C^{(2)}$, and show that this set is mapped by M into itself; by Schauder's lemma M will have a fixed point. We indicate a choice of the set K and sketch the proof of the fact that M maps K into itself.

Let

$B_c = \{\Delta, \dot{\Delta} \in C^{(2)}(0, 1) \mid \Delta$ satisfies (BC1). $|\Delta|, |\Delta_x|, |\Delta_{xx}| \leq c$; Δ_{xx} and $\dot{\Delta}_{xx}$ are Lipshitz functions each with Lipshitz constant c. $\dot{\Delta}_x(0) = \dot{\Delta}_x(1) = 0$, $|\dot{\Delta}|, |\dot{\Delta}_x|, |\dot{\Delta}_{xx}| \leq c.\}$

B_c is a convex set and compact in $C(0, 1)$. As in part *a*), the inequality $0 \leq \dot{s} \leq c$ is preserved in time if c is chosen large enough. Thus we set $K = [0, c] \times B_c$. We now verify that $MK \subset K$ for c sufficiently large.

Rewrite Eq. (5.17) so as to obtain homogeneous boundary conditions for Δ. Take

$$p(x) = \tfrac{1}{2}(H + I)x^2 - \tfrac{1}{2}H(x - 1)^2,$$

and set

$$v = \Delta - p(x).$$

Now v satisfies

$$\left.\begin{aligned} v_x|_{x=0,1} &= 0 \\ \dot{v}_x|_{x=0,1} &= 0, \end{aligned}\right\} \tag{BC2}$$

and

$$v_{tt} + \sigma v_t - v_{xx} + \sin(v + p + s) - \int_0^1 \sin(v + p + s)\, dx + I = 0, \tag{5.17}'$$

or, as a system

$$\left.\begin{aligned} \dot{v} &= w, \\ \dot{w} &= -\sigma w + v_{xx} + f(v, s). \end{aligned}\right\} \tag{5.17}''$$

Set

$$\begin{pmatrix} v \\ w \end{pmatrix} = u, \begin{pmatrix} 0 & I \\ \partial^2 & -\sigma I \end{pmatrix} = A \quad (\partial \text{ denotes } x\text{-differentiation}), \quad \begin{pmatrix} 0 \\ f \end{pmatrix} = F,$$

and obtain (4.1b) in the form

$$\dot{u} = Au + F, \tag{5.20}$$

where u satisfies the homogeneous boundary conditions (BC2). (5.20) has a general

solution of the form

$$u(x, t) = \exp(At)u(x, 0) + \int_0^t \exp(A(t-\tau))F(u(x, \tau))\, d\tau. \tag{5.21}$$

Let B_c^0 be B_c with BC1 replaced by the homogeneous boundary conditions, (BC2).

To prove that $MK \subset K$ it suffices to show that if $u(x, 0) \in B_c^0$, then $u(x, \tau) \in B_{c/2}^0$ where c can be chosen arbitrarily large and where τ depends only on c, but not on the initial data. We will use the following information about A restricted to B_c^0 (without proof): if $u \in B_c^0$ and $t > \tau = \tau(c)$, then

$$\begin{aligned} &||\exp(At)\partial_x{}^j u|| \leq L \exp(-\alpha t)\, ||\partial_x{}^j u||, j = 0, 1, 2, \text{ where } ||\cdot|| \\ &\text{is the } C([0, 1])\text{-norm and } \exp(At)\partial_x{}^2 u \text{ is a Lipshitz function with a} \\ &\text{Lipshitz constant } L \exp(-\alpha t)\ \alpha > 0,\ \alpha \text{ and } L \text{ depend only on } c. \end{aligned} \tag{5.22}$$

It remains only to observe that (5.22) applied to (5.21) readily imply that

$$u(x, 0) \in B_c^0 \Rightarrow u(x, T) \in B_{c/2}^0$$

if c is chosen large enough, T depends only on c. This concludes the proof of part b) and of Theorem 5.1.

Appendix. Proofs of the assertions of Sec. 3.1.

Proof of Proposition 3.1. For $I > 1$ the absence of singular points is obvious. The existence of a running periodic solution is obtained from the following geometric construction (consult Fig. A.1).

For $y \geq 2(1 + I)/\sigma$ we have $\dot{y} < c_2 < 0$, and for $y \leq (I - 1)/2\sigma > 0$ we have $\dot{y} > c_2 > 0$. Here c_1 and c_2 are appropriate constants. Moreover, in the strip

$$\frac{I-1}{2\sigma} \leq y \leq 2\frac{I+1}{\sigma}, \qquad \dot{x} \geq \frac{I-1}{2\sigma} > 0. \tag{A.1}$$

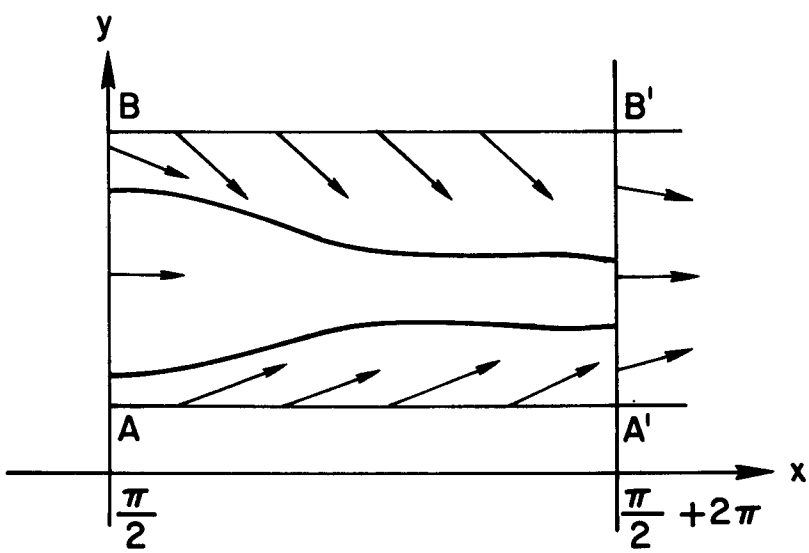

FIG. A.1. Solutions of system (3.1) map the segment AB into the segment $A'B'$.

Thus each trajectory starting on the segment AB will reach $A'B'$ (see Fig. A.1) in finite time ($\leq 2\pi(I-1)/2\sigma)^{-1}$). Moreover, the trajectories intersect AB and $A'B'$ transversally. Thus we have a continuous, smooth map $M: AB \to A'B'$, taking each point from AB along the phase flow into $A'B'$.

Thus, M has a fixed point. This proves the existence of a running periodic solution.

To prove the exponential stability and uniqueness of running periodic solution we begin by noting that since $\dot{x} = y > 0$ in the strip $AA'B'B$, and since the trajectories, once in the strip, never approach the x-axis, we may write (A.1) as

$$\frac{dy}{dx} = -\sigma + \frac{I - \sin x}{y}. \tag{A.2}$$

It suffices to show that if $y(x, y_0)$ is a solution of (A.2) with $y(0, y_0) \in AB$, then

$$My_0 = y(\pi, y_0)$$

has a positive derivative which is less than 1: i.e. for some constants α and β, we have

$$0 < \alpha < y_{y_0}'(2\pi + \pi/2, y_0) < 1 - \beta, \qquad 0 < \beta < 1.$$

(The positivity of y_{y_0}' follows from consideration of M^{-1} and its boundedness on $M(AB)$.) Write (A.2) as $dy/dx = f(x, y)$. With $y = y(x, y_0)$, we differentiate this equation with respect to y_0:

$$\frac{d}{dx} y_{y_0}' = f_y' \cdot y_{y_0}'. \tag{A.3}$$

Note that there exists a positive constant c so that $f_y' = -(I - \sin x)/y^2 \leq -c < 0$ in the strip, since y is bounded therein. Thus, by using $y_{y_0}'(\pi/2) = 1$, (A.3) yields

$$y_{y_0}'(x) = y_{y_0}'\left(\frac{\pi}{2}\right) \exp\left(\int_0^x f_y'\, dx\right) \leq \exp(-cx).$$

Finally,

$$M'(y_0) = y_{y_0}'\left(2\pi + \frac{\pi}{2}\right) < \exp(-2\pi c) < 1.$$

Thus every solution starting on AB tends exponentially to the running periodic solution in the sense that for any two solutions (x_1, y_1) and (x_2, y_2) starting on AB,

$$y_1(x) - y_2(x) = O(\exp(-cx)).$$

Moreover, any solution starting outside the strip (i.e. for $y \leq (I-1)/\sigma$ or $y \leq 2(I+1)/\sigma$) eventually runs into the strip. This completes the proof of Proposition 3.2.

Proof of Remark 3.1. The smooth dependence of V on σ and I is clear from the fact that

1) the map $M \equiv M_{\sigma, I}(y)$ depends smoothly on σ, I.

2) $\frac{d}{dy} M_{\sigma, I}(y) < 1$.

1) and 2) imply that the fixed point of $M_{\sigma, I}$ (through which the running periodic solution passes) depends on σ, I smoothly.

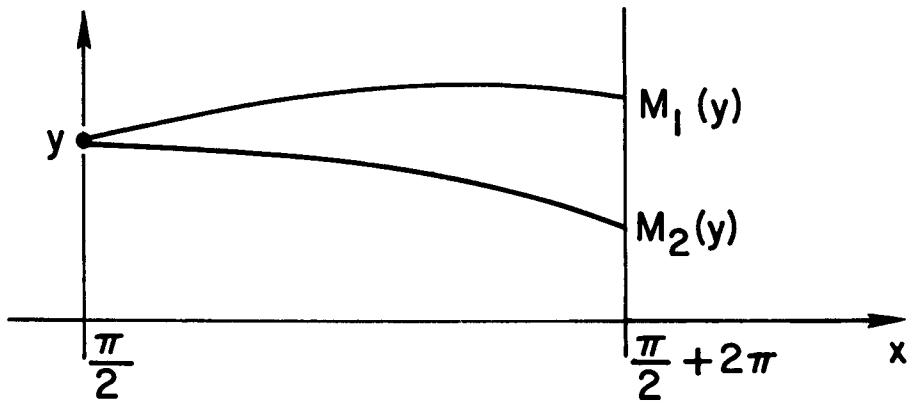

FIG. A.2.

It remains to prove the monotonicity statements. We note that increasing σ or decreasing I (while still keeping $I > 1$) both have the same effect of decreasing $M_{\sigma, I}(y)$. Omitting the simple details, we illustrate this statement in Fig. A.2. M_2 corresponds to a larger σ or a smaller I. Let $\sigma_1 \leq \sigma_2$, $I_1 \leq I_2$, and suppose that at least one of these inequalities is strict. Two trajectories corresponding respectively to the fields

$$\dot{x} = y$$
$$\dot{y} = -\sigma_i y + I_i - \sin x, \qquad i = 1, 2, \pi/2 \leq x \leq 5\pi/2,$$

both starting at $(\pi/2, y)$ (in the upper half-plane), satisfy

$$y_2(x) < y_1(x), \qquad \frac{\pi}{2} < x \leq \frac{5\pi}{2}.$$

This follows directly from the fact that the vector field for $i = 1$ has a larger vertical component:

$$-\sigma_1 y + I_1 - \sin x > -\sigma_2 y + I_2 - \sin x. \tag{A.4}$$

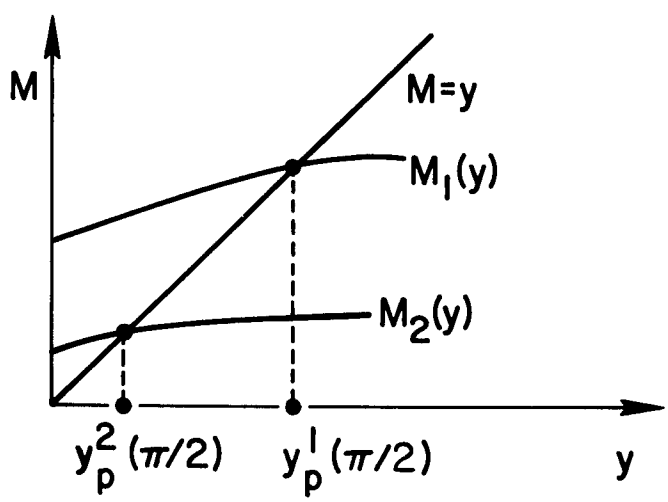

FIG. A.3.

Thus $M_1(y) > M_2(y)$, which in turn implies the same relation between the fixed points of M_1 and M_2; Fig. A.3 illustrates this point. In other words, the running periodic solutions $y_p^1(x)$, $y_p^2(x)$ satisfy

$$y_p^1(x) > y_p^2(x) \tag{A.5}$$

for $x = \pi/2$. This and (A.4) imply the validity of (A.5) for all x.
Finally, since

$$T = \int_{\pi/2}^{5\pi/2} dt(x) = \int \frac{dx}{y_p(x)},$$

we see that

$$V(\sigma_1, I_1) = \frac{2\pi}{T_1} = 2\pi \Big/ \int \frac{dx}{y_p^1(x)} > 2\pi \Big/ \int \frac{dx}{y_p^2(x)} = V(\sigma_2, I_2).$$

This completes the proof of Remark 3.1.

Proof of Proposition 3.2. To begin we list the main steps 1) – 4) of the argument.

Step 1) We restrict our attention to $x \in [\pi/2, (\pi/2) + 2\pi]$, $y \geq 0$, and note that the vector field

$$\dot{x} = y, \qquad \dot{y} = -\sigma y + 1 - \sin x$$

is 2π-periodic in x.

We demonstrate the existence of a solution, which we denote either by $(x_h(t), y_h(t))$ or by $y_h(x)$ (whichever is more convenient), such that for $t \to \infty$ $(x_h, y_h) \to (\pi/2 + 2\pi, 0)$ at an angle π-$\tan^{-1}\sigma$ (see Fig. A.4). In other words, $y_h'(5\pi/2 - 0) = -\sigma$. Moreover, any trajectory passing above this solution leaves the strip $\pi/2 \leq x \leq 5\pi/2$, $y \geq 0$ for some t through the right "wall". (In the upper half plane the horizontal component of the field is positive and on the horizontal axis the field is pointed up.) In other words, if $y(x) > y_h(x)$ for some $\pi/2 < x < 5\pi/2$, then $y(\pi/2 + 2\pi) > 0$. Thus $y_h(x)$ is the highest solution that tends to 0 as $x \to (5\pi/2) - 0$.

Step 2) Depending on whether $y_h(x)$ emanates from (see Figs. 3.2, A.6, A.10 and A.15)

a) the bottom of the strip, i.e. from $(x, 0)$ with $x \in (\pi/2, 5\pi/2)$, specifically for some $t = t_0$, $x(t_0) \in (\pi/2, 5\pi/2)$, $y(t_0) = 0$;

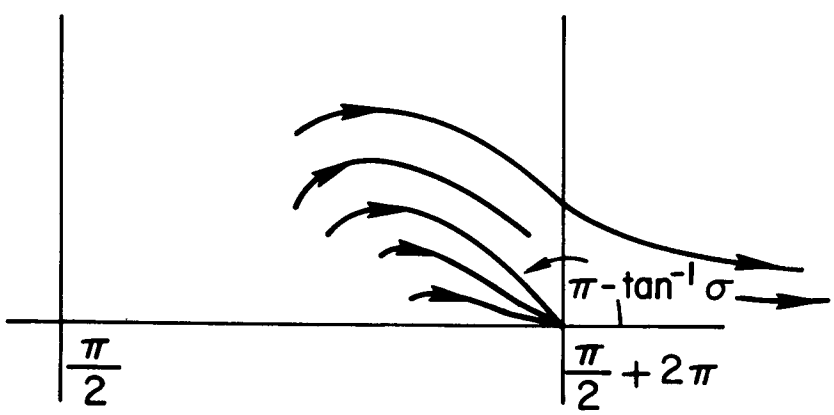

FIG. A.4.

b) the left wall of the strip: $(\pi/2, y)$, $y > 0$, i.e. $y_h(\pi/2) > 0$;

c) the left corner: $(\pi/2, 0)$, i.e. $y_h(\pi/2) = 0$,

there are three corresponding cases (see Fig. 3.2):

i) There is one running periodic solution which is, moreover, exponentially stable;

ii) There is no running periodic solution; all trajectories tend to one of the singular points;

iii) There is no running periodic solution, the phase plane is split by $y_h(x)$ (2π-periodically continued in x) into two regions as in Fig. 3.2 (*iii*).

Step 3) There exist values of σ such that the alternatives a), b) of Step 2 hold:

For a) to hold, σ must be sufficiently small (we give a rough estimate),

For b) to hold, σ has to be large enough ($\sigma > 2$ turns out to be sufficient).

Step 4) The values of σ described by a) and b), Step 2 cover the whole set of real positive numbers except one separating point $\sigma = \sigma_0$, which corresponds to the alternative c) (Step 2).

We now begin the proofs.

Step 1. To investigate the flow

$$\dot{x} = y, \qquad \dot{y} = -\sigma y + 1 - \sin x$$

near the rest point

$$x = \frac{\pi}{2} + 2\pi$$

$$y = 0 \text{ (the same, of course, for } \frac{\pi}{2} + 2\pi n),$$

we introduce $z = x - 5\pi/2$ to obtain

$$\dot{z} = y, \qquad \dot{y} = -\sigma y + 1 - \cos z. \tag{A.6}$$

Now the rest points are $z = 0(1 + 2\pi n)$, $y = 0$; we consider $n = 0$ without loss of generality. Introduce the polar coordinates $z = r\cos\phi$, $y = r\sin\phi$, and write $1 - \cos z = (z^2/2)(1 + 0(z^2))$. (3.6) becomes

$$\dot{\phi} = -\sin\phi\cos\phi\,(\sigma + \tan\phi) + \tfrac{1}{2} r\cos^2\phi(1 + O(r^2\cos^2\phi))$$

$$\dot{r} = r\sin\phi\cos\phi\,(1 - \sigma\tan\phi + \tfrac{1}{2} r\cos\phi\,(1 + O(r\cos\phi))). \tag{A.6}'$$

(A.6)′ has the rest point $\phi = \phi_0 = \pi - \tan^{-1}\sigma$, $r = 0$. Linearizing this system near that point, we obtain

$$\dot{\tilde{\phi}} = c_1\tilde{\phi} + c_2\tilde{r}, \qquad \dot{\tilde{r}} = -c_3\tilde{r},$$

where the c_1, c_2, c_3 are positive constants. The matrix of the linear system has two real eigenvalues of opposite sign: $\lambda_1 = c_1$, $\lambda_2 = -c_3$. Thus $\tilde{r} = \tilde{\phi} = 0$ is a hyperbolic singular point.

The flow of the nonlinear system (A.6)′ has the same qualitative behavior near the point $r = 0$, $\phi = \phi_0 = \pi - \tan^{-1}\sigma$. In particular, there is a stable manifold S, tending (as $t \to \infty$) to $\phi = \phi_0$, $r = 0$. All the trajectories to the left (right) of S near S, in the strip $0 \le r \le r_0$, r_0 small enough, deflect to the left (right) (see Fig. A.5). Moreover, any trajectory starting to the left of S with $\frac{\pi}{2} < \phi < \pi$, $0 \le r \le r_0$ crosses the line $\phi = \pi/2$ after some finite time. Indeed, from the second equation in (A.6)′ it follows that $\dot{r} < 0$ in the strip $0 < r < r_0$ (r_0 not too large). Therefore any trajectory starting inside the (curvilinear) rectangle

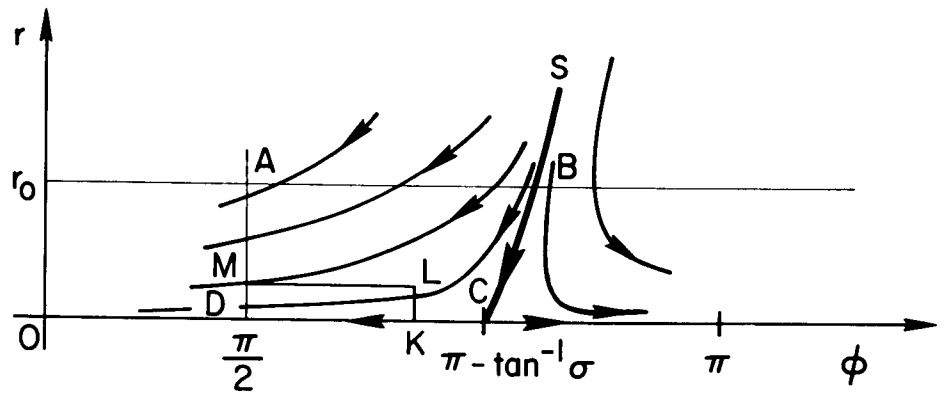

FIG. A.5.

$ABCD$ in Fig. A.5 either leaves through AD (which we want to prove) or tends to DC. The last, however, is impossible since, first, such a trajectory does not approach C too closely (C is a hyperbolic point), and second, if it enters a small neighborhood of DC in the thin rectangle $DKLM$ with small altitude DM (away from C), its speed $\dot{\phi} < -\phi < 0$, as is easily seen from the first equation in (A.6)', so it cannot stay there indefinitely.

Translating these observations to the (x, y)-plane, we obtain the assertion of Step 1: the trajectory corresponding to S is $y_h(x)$; $y_h(x) \to 0$ as $x \to 5\pi/2$,

$$y_h'\left(\frac{5\pi}{2}\right) = \lim_{x \to 5\pi^-/2} \frac{y_h(x) - y_h\left(\frac{5\pi}{2}\right)}{x - \frac{5\pi}{2}} = \lim_{x \to 5\pi^-/2} \frac{y_h(x)}{x - \frac{5\pi}{2}} = \lim_{\phi \to \pi - \tan^{-1}\sigma} \frac{r \sin \phi}{r \sin \phi} = -\sigma.$$

Moreover, in a neighborhood of the point $(5\pi/2, 0)$, $y_h(x)$ is the highest trajectory tending to that point. But then the same is obviously true for (not only a small neighborhood, but) all $y \geq 0$ and $x \in [\pi/2, 5\pi/2]$.

Step 2. a) Assume that $y_h(x)$ crosses the interval

$$\pi/2 < x < 5\pi/2, \qquad y = 0$$

(see Fig. A.6), and show that there exists an exponentially stable running periodic solution. To do this, and for further use, we will need the following auxiliary proposition.

PROPOSITION 3.4. There is a unique trajectory $(y_e(t), x_e(t))$ (or $y_e(x)$) of the vector field (3.1), $I = 1$, in the strip, $x \in [\pi/2, 5\pi/2]$, $y \geq 0$, emanating from $(\pi/2, 0)$:

$$\lim_{t \to -\infty} y_e(t) = 0, \qquad \lim_{t \to -\infty} x_e(t) = \frac{\pi}{2} + 0.$$

Proof: Consider the segment AB (see Fig. A.7) chosen to be transversal to the flow; transversality is assured if we choose AB to be free of rest points and such that the slope of AB is less than $-\sigma$. To see this, take $CB < 2\pi$ and let the slope of $AB = -s(< -\sigma)$. Transversality of AB to the flow means that the normal to AB is not perpendicular to the flow, i.e. $(s, 1)\cdot(y, -\sigma y + 1 - \sin x) \neq 0$ but that

$$(s - \sigma)y + 1 - \sin x > 0$$

holds for (x, y) lying on AB. Moreover, with our choice of B ($CB < 2\pi$), the only singular point in ABC is C.

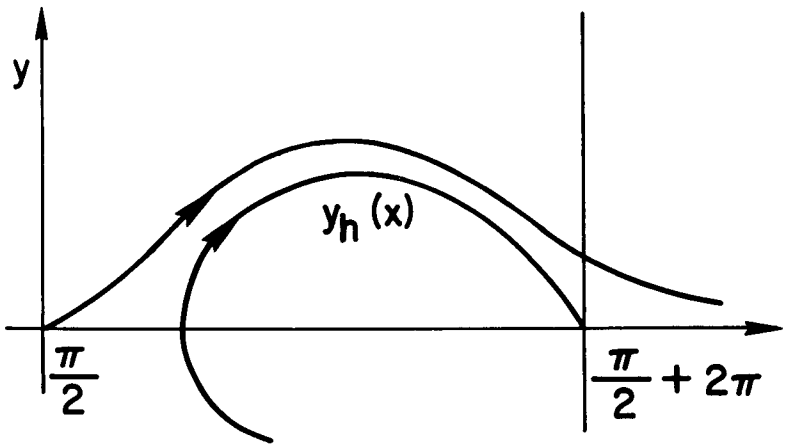

FIG. A.6.

Now consider the two sets of points on AB whose trajectories emanate from the sides AC and CB respectively. These sets are both nonempty, nonintersecting, and open (in AB). Hence, the complement (in AB) of the union of these two sets is nonempty. It consists of the trajectories emanating from C.

It is easy to see, moreover, that there is only one such trajectory. Indeed, the existence of two such would allow us to construct a curvilinear triangle Δ as shown in Fig. A.8. With increasing time, this triangle will stretch into a larger triangle Δ' contradicting the fact that the divergence of the flow is negative $(-\sigma)$.

This completes the proof of the auxilliary Proposition 3.4. We return to the proof of a) of Step 2.

The trajectory $y_e(x)$ emanating from $x = \pi/2$, $y = 0$ will pass above the trajectory $y_h(x)$, and thus by the maximality property of $y_h(x)$, $y_e(5\pi/2) > 0$. Thus the mapping M, which takes $y = y(\pi/2)$ into $y(5\pi/2)$, takes $y \geq 0$ into itself.

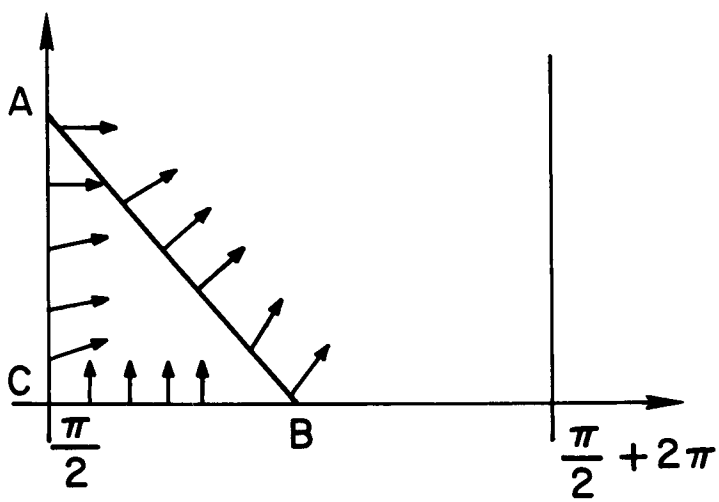

FIG. A.7.

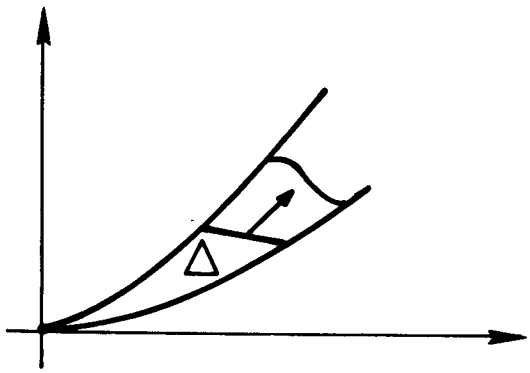

FIG. A.8.

Similar to the case $I > 1$, we have

$$M'(y) = \exp\left[-\int_{\pi/2}^{5\pi/2} \frac{1-\sin x}{y^2}\,dx\right] \leq \exp(-c) < 1,$$

for some positive constant c; this implies the existence of a unique fixed point of M (see Fig. A.9). Thus, the existence of a running periodic solution, and its exponential stability is established. This completes case a).

b) Assume $y_h(0) > 0$; show that there is no running periodic solution. As before, we construct the map

$$M: \left[y_h\left(\frac{\pi}{2}\right), \infty\right] \to [0, \infty]$$

(see Fig. A.10). Again, $M'(y) < 1$, and therefore M has no fixed points (see Figure A.11).

Since M' is strictly less than unity, there exists a constant c such that $0 < M' < c < 1$, $y > 0$. Since also $M(y_h(\pi/2)) = 0$, then for any fixed $y > 0$, there exists an n such that the n-fold iterate of M, $M \circ \cdots \circ M(y) = 0$ for $n = n(y)$ large enough. Thus, any trajectory in

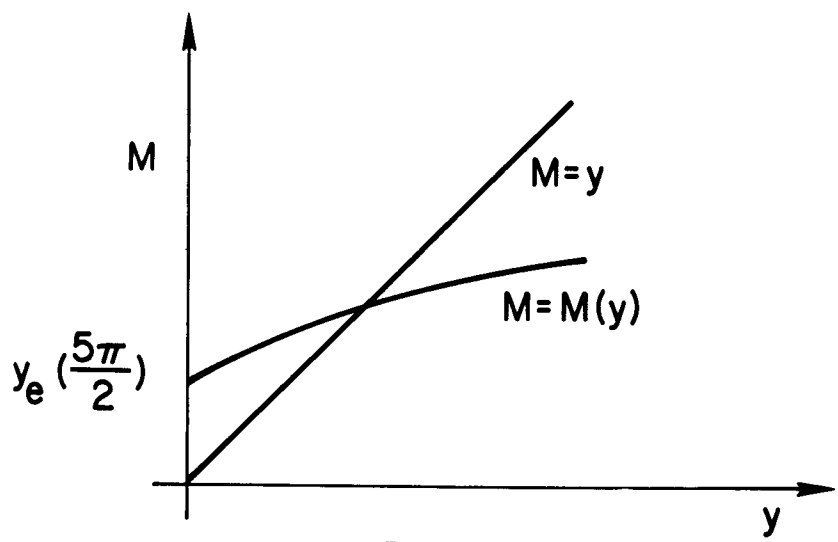

FIG. A.9.

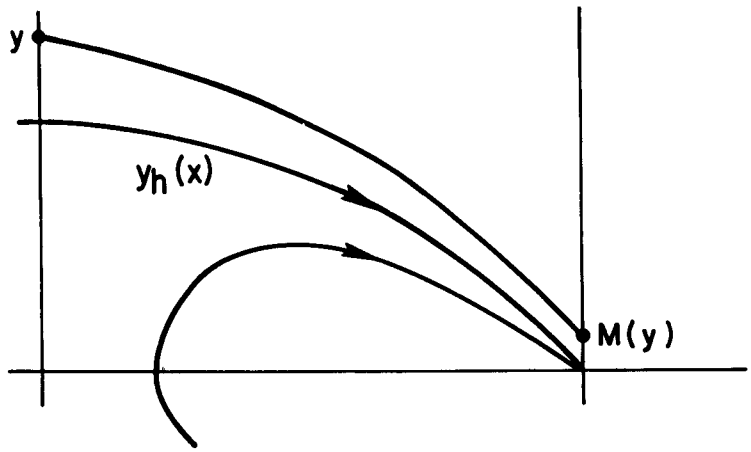

FIG. A.10.

the upper half-plane tends to some rest point. For the lower half-plane this fact is obvious. This completes case b).

c) When $y_h(\pi/2) = 0$ the plane is split into two parts by $y_h(x)$ (continued 2π-periodically in x). Clearly, all trajectories originating in the lower part tend to some rest point (see Fig. 3.2 (iii)).

Consider the map M:$[0, \infty) \to [0, \infty)$ defined as before. As before, $0 < M'(y) < c < 1$, and $M(0) = 0$. This implies the existence of only one fixed point of M, namely $y = 0$ (see Fig. A.12). Since $(\pi/2, 0)$ is a rest point this fixed point does not correspond to a running periodic solution. Moreover the n-fold iterate of M, $M \circ \cdots \circ M\, y \Rightarrow 0$ as $n \to \infty$, which shows that any trajectory from the upper part of the plane tends to the boundary between the two parts, never reaching a singularity in finite time. This completes case c) and with it Step 2.

Step 3. 1) We show that for σ small enough $y_h(x_0) = 0$, $\pi/2 < x_0 < 5\pi/2$, which by Step 2, a) implies the existence of a running periodic solution.

Proof: $y_h(x_0) = 0$ is equivalent to $y_e(5\pi/2) > 0$ (see Fig. A.13). We omit the simple

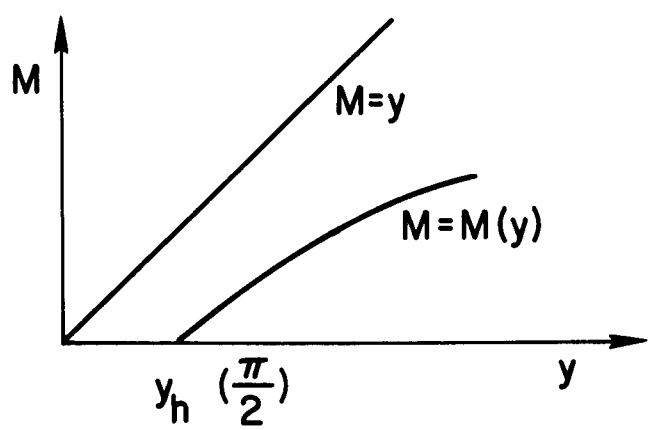

FIG. A.11.

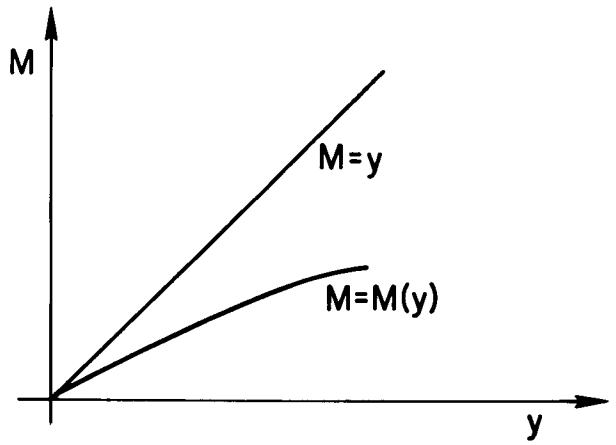

FIG. A.12.

argument based on maximality property of y_h and the uniqueness of $y_e(x)$, so that we prove only the latter inequality. To that end define the energy of the pendulum:

$$E(x) = \frac{\dot{x}^2}{2} + \int_{\pi/2}^{x} \sin x\, dx = \dot{x}^2/2 - \cos x. \tag{A.7}$$

Note that

$$dE/dt = (\ddot{x} + \sin x)\dot{x} = (1 - \sigma\dot{x})\dot{x} = (dE/dx)(dx/dt),$$

which shows that

$$dE/dt = 1 - \sigma\dot{x}. \tag{A.8}$$

For $y_e(x)$ we have $E_0 \equiv E(y_e(\pi/2)) = 0$ and $E_1 \equiv E(y_e(5\pi/2)) = y_e^2(5\pi/2)2$, and it is enough to show that $E_1 > 0$ (see Fig. A.13). (y_e cannot be less than zero for $\pi/2 < x < 5\pi/2$, since the vector field points upward on $y = 0$.) From (A.8),

$$E_1 = \int_{\pi/2}^{5\pi/2} (1 - \sigma\dot{x}_e)\, dx = 2\pi - \sigma \int_{\pi/2}^{5\pi/2} y_e dx.$$

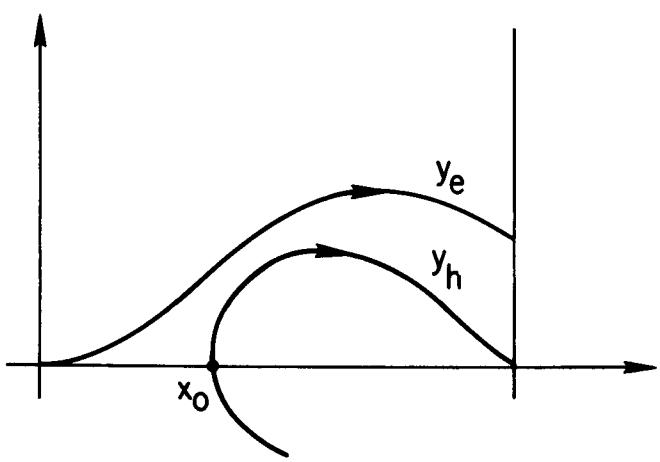

FIG. A.13.

Thus the condition $y_e(5\pi/2) > 0$ sufficient for the existence of a running periodic solution may be expressed as

$$\sigma \int_{\pi/2}^{5\pi/2} y_e(x)\, dx < 2\pi. \tag{A.9}$$

To find σ for which (A.9) is true we compare our system with the frictionless pendulum:

$$\dot{x} = y, \qquad \dot{y} = 1 - \sin x. \tag{A.10}$$

The unique solution emanating from $(\pi/2, 0)$ persists for $\sigma = 0$, and we call it $y_e^0(x)$. We will show that

$$y_e^0(x) > y_e(x), \qquad \pi/2 < x < 5\pi/2,$$

but first we will use this fact to obtain a sufficient condition implying (A.9).

We note that for (A.9) to hold it is enough to take

$$\sigma < \frac{2\pi}{\int y_e^0(x)dx}.$$

$y_e^0(x)$ can easily be found from the conservation of energy of (A.10):

$$y_e^2/2 - \cos x = x + c.$$

We find that $c = -\pi/2$ by letting $x = \pi/2$ and recalling that $y_e(\pi/2) = 0$. Thus $y_e^0(x) = (2(\cos x + x - \pi/2))^{1/2}$. Then (A.9) may be replaced by the following sufficient condition for the existence of a running periodic solution:

$$\sigma < 2\pi \Big/ \int_{\pi/2}^{5\pi/2} \left(2\left(\cos x + x - \frac{\pi}{2}\right)\right)^{1/2} dx$$

Now we return to show that $y_e^0(e) > y_e(x)$ for $\pi/2 < x < 5\pi/2$. We note that in the upper half-plane

$$1 - \sin x > -\sigma y + 1 - \sin x, \tag{A.11}$$

i.e. the auxiliary vector field has larger vertical components. Assume (the contrary), that for some $x_0 \in (\pi/2, 5\pi/2)$, $y_e^0 < y_e$. Then the same must hold for all $x \in (0, x_0)$ by virtue of (A.11): if the equality holds for some $\xi < x_0$, then $y_e^0 > y_e$ for $x > \xi$ (and $x < 5\pi/2$).

Now consider the trajectory $y(x)$ of the flow with $\sigma > 0$ passing through this point. We restrict our attention to $0 \le x \le x_0$ (see Fig. A.14). On the one hand, this trajectory has to cross the x-axis in the interval $\pi/2 < x < x_0$ since $y(x) < y_e(x)$, and $y_e(x)$ is the *unique* trajectory emanating from $(\pi/2, 0)$. On the other hand, it cannot cross $y_e^0(x) > 0$ for $x < x_0$, by the same argument as before, and $y_e(x) > y_e^0(x) > 0$ for $\pi/2 < x < x_0$. The contradiction proves the assertion.

Step 3. 2) We show that for σ large enough $y_h(\pi/2) > 0$, so that there is no running periodic solution according to b), Step 2.

We show that for σ large enough, $y_h(x_0) > 2/\sigma$ for some $\pi/2 < x_0 < 5\pi/2$; this implies our assertion since $y_h(x)$ has to satisfy $y_h(x) > 2/\sigma > 0$ for $\pi/2 \le x \le x_0$. Indeed, if for some $x \in [\pi/2, x_0]$, $y_h(x) < 2/\sigma$, then $y_h(x_0) < 2/\sigma$ since the vector field in $y = 2/\sigma$ has a negative vertical component:

$$\dot{y} = -\sigma y + 1 - \sin x < -2 + 1 - \sin x < 0.$$

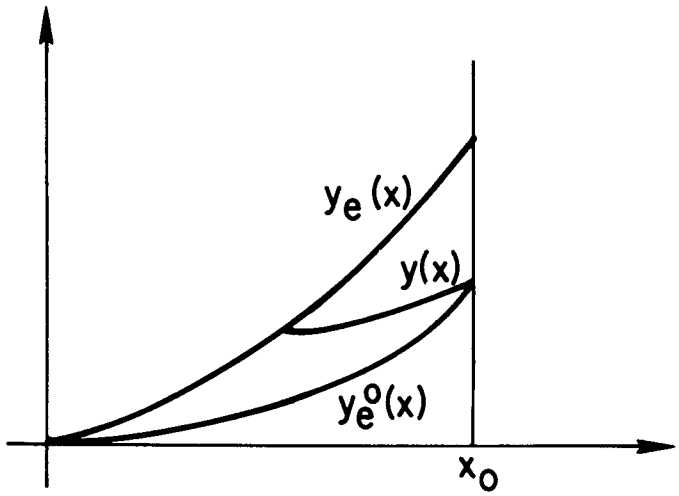

FIG. A.14.

To prove the existence of such x_0, we consider an auxiliary (linear) field together with our system:

$$\dot{z} = y$$

$$\dot{y} = -\sigma y + (1 - \cos z) \left(z = x - \frac{5\pi}{2}\right)$$

for $y \geq 0$, and

$$\dot{\xi} = \eta, \qquad \dot{\eta} = -\sigma\eta - \xi, \tag{A.13}$$

for $\eta \geq 0$.

The auxiliary system is majorized by (A.12) for $-1 \leq z \leq 0$:

$$1 - \cos z < z^2/2 < -z.$$

It suffices to show that (A.13) has a solution $\eta(\xi)$ such that
a) $\eta \to 0^+$ for $\xi \to 0^-$, b) $\eta(\xi) < y_h(\xi)$, $-1 \leq \xi \leq 0$, c) $\eta(-1) > 2/\sigma$.
a) This follows immediately from the fact that

$$\lambda_{1,2} = -\left(\frac{\sigma}{2} \pm \left(\frac{\sigma^2}{4} - 1\right)^{1/2}\right) < 0 \qquad (\sigma > 2)$$

are the eigenvalues of the matrix of (A.13), so that $\eta = \lambda\xi$ ($\lambda = \lambda_1$ or λ_2) is a suitable trajectory.

b) Take $\eta(\xi) = \lambda_2\xi$. Since $\lambda_1 = -((\sigma/2) + ((\sigma^2/4) - 1)^{1/2}) > -\sigma$, the (straight line) trajectory $y = \lambda_1 z$ of (A.13) is below $y_h(z)$, for small z. This follows from the fact that $y_h(z)$ approaches $z = y = 0$ at an angle π-$\tan^{-1}\sigma$. But then $y_h(z) > \lambda_1 z$ for $-1 \leq z \leq 0$, where (3.14) holds. This proves b).

c) For $z = -1$,

$$\eta(-1) = -\lambda_1 = \frac{\sigma}{2} + \left(\frac{\sigma^2}{4} - 1\right)^{1/2} > \frac{2}{\sigma}, \qquad \sigma > 2.$$

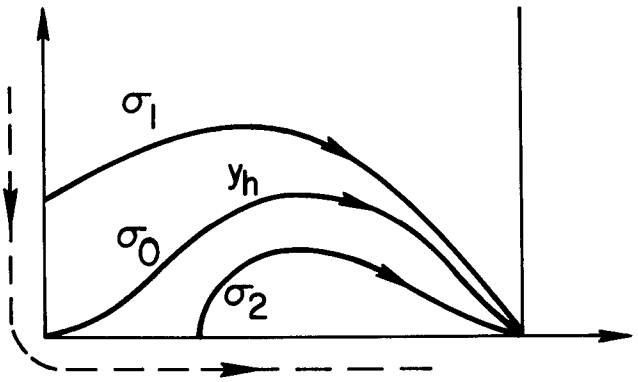

FIG. A.15.

This completes Step 3.

Step 4. Here we show that

1) As σ decreases from $+\infty$ to 0, the point of intersection of the trajectory $y_h(x)$ with the axis $x = \pi/2$, $y \geq 0$ or with $\pi/2 \leq x \leq 5\pi/2$ moves continuously and without change of direction, as is shown in Fig. A.15. This implies that $y_h(\pi/2) = 0$ for some $\sigma_0 \in (0, \infty)$.

2) There exists only one $\sigma(=\sigma_0)$ such that $y_h(\pi/2) = 0$.

Proof of 1). Assume, first, $y_h(\pi/2) > 0$. Since $y_h(x)$ approaches $(x = 5\pi/2, y = 0)$ at an angle $\pi - \tan^{-1}\sigma$, the trajectories $y_h(x)$ with larger σ are higher than those with smaller σ—at least for $(5\pi/2) - \epsilon < x < 5\pi/2$, ϵ small. But then the inequality $y_h^{\sigma_1}(x) > y_h^{\sigma_2}(x)$, $\sigma_1 > \sigma_2$ is preserved for all $\pi/2 < x < 5\pi/2$. (Indeed, if for some $\pi/2 < x_0 < 5\pi/2$, $y_h^{\sigma_1}(x_0) = y_h^{\sigma_2}(x_0)$, then $y_h^{\sigma_1}(x) < y_h^{\sigma_2}(x)$ for $x_0 < x < 5\pi/2$ since the vector field with larger σ has a smaller vertical component.) This proves that $y_h^{\sigma}(\pi/2)$ depends monotonically on σ. The proof of the monotonic dependence of the point of intersection of $y_h^{(x)}$ with the horizontal axis is completely analogous.

We omit the simple proof of *continuous* dependence of intersection points on σ—this proof is based on the behavior of $y_h^{(x)}$ near $(5\pi/2, 0)$ and the theorem on continuous dependence of solutions on initial data.

3) There exists at least one σ_0 such that

$$y_h^{\sigma_0}(\pi/2) = 0.$$

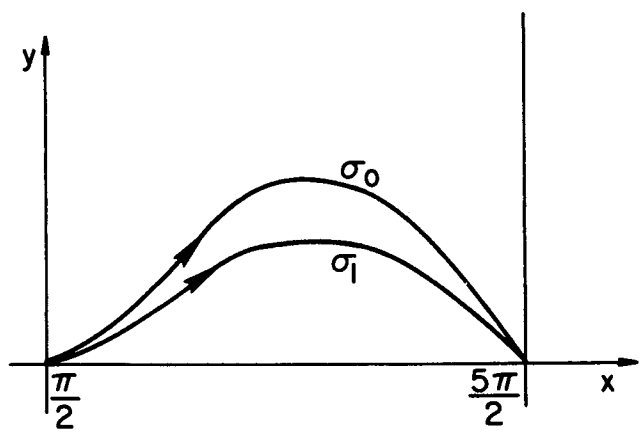

FIG. A.16.

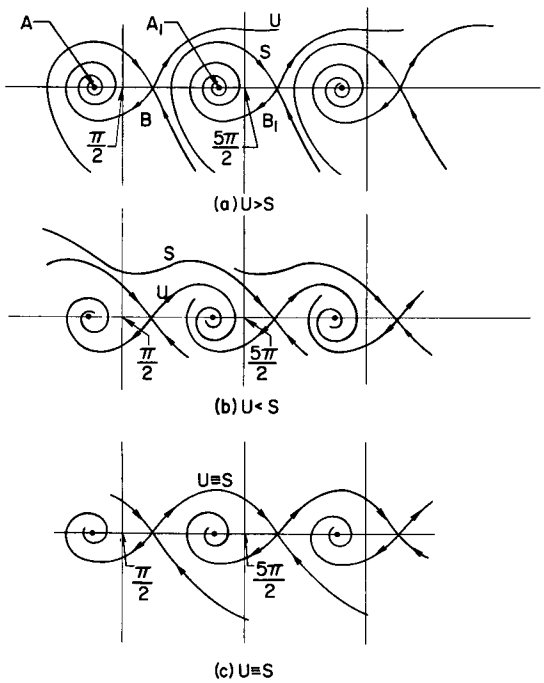

FIG. A.17. Phase plane diagrams of (3.1) for $I = 1$. These are classified by the relation between the unstable manifold U and the stable manifold S.

To show the uniqueness of such σ_0, assume that there are two trajectories, $y_h^{\sigma_0}$, $y_h^{\sigma_1}$, both vanishing at $x = \pi/2$ (see Fig. A.16) ($\sigma_0 > \sigma_1$).

A contradiction is obtained by noting that, on the one hand, $y_h^{\sigma_0}(x) > y_h^{\sigma_1}(x)$, since this is the case near and to the left of $5\pi/2$, and thus for all $\pi/2 < x < 5\pi/2$; on the other hand, $y_h^{\sigma_0}(x) < y_h^{\sigma_1}(x)$ by the argument given in Step 3, 1). This completes the proof of Step 4 and of Proposition 3.2.

Comments on Proposition 3.3. We omit the proof of Proposition 3.3 since it is similar to the case $I = 1$. Instead we give a description of phase plane of the system for the cases i), ii), iii) (see Fig. A.17).

There are two singular points (modulo 2π): $A \equiv (\sin^{-1} I, 0)$ and $B \equiv (\pi - \sin^{-1} I, 0)$. The first point is stable (a focus or node), and the second is a saddlepoint; the complicated singular point for $I = 1$ (which is analyzed in the proof in Step 1 of the proof of Proposition 3.2) bifurcates into these two singular points as I becomes less than one.

The role of $y_e(x)$ (in the $I = 1$ case) is replaced by an unstable manifold (denoted by U in Fig. A.17) of the saddlepoint B. The role of $y_h(x)$ is replaced by the stable manifold S of a saddlepoint B_1 located 2π to the right of B.

The alternatives i), ii), iii) of Proposition 3.3 hold when correspondingly:

i) S lies below U,
ii) S lies above U,
iii) S coincides with U.

In the case iii) the plane is split into two parts by $S \equiv U$ (continued 2π-periodically in x).

References

[1] Y. Imry and P. Marcus, *Nonlinear effects in coupled Josephson devices,* Proceedings of the 1975 Stanford Applied Superconductivity Conference.

[2] Y. Imry and L. S. Schulman, *Qalitative theory of nonlinear behavior of coupled Josephson junction,* to appear.

[3] D. N. Landberg, D. J. Scalapino and B. N. Taylor, *The Josephson effects,* Scientific American, **21**, 30–39 (May 1966).

[4] W. Liniger and F. Odeh, *Perturbation solutions of the Josephson phase equation,* to appear.

[5] J. Matisoo, *Josephson-type superconductive tunnel junctions and applications,* IEEE Transactions on Magnetics, **5**, 848–873 (1969).

[6] F. Odeh, *On existence, uniqueness and stability of solutions of the Josephson phase equation,* to appear.

[7] C. S. Owen and D. J. Scalapino, *Vortex structure and critical currents in Josephson junctions,* Pht. Rev., **164**, 538–544 (1967).

[8] J. M. Rowell, Phys. Rev. Letters **11**, 200 (1963).

[9] J. J. Stoker, *Nonlinear vibrations in mechanical and electrical systems*, Interscience, N.Y., 1950

[10] F. Tricomi, *Integrazione di un'equazione differenzale presentasi in elettrotecnica,* Ann. Sc. Norm. Sup. Pisa **2** (1933)